Anisotropic Energy Gap in Superconducting White Tin: Semiempirical Approach

ALAN J. BENNETT*†
Cavendish Laboratory, Cambridge University, Cambridge, England
(Received 10 June 1966)

The anisotropic energy gap in superconducting tin is found in terms of an expansion in tetragonal harmonics. The anisotropy coefficients are determined from a selection of Zavaritskii's single-crystal tunneling data by means of some results of a previous calculation of the anisotropic gap in lead. In particular, generalization of the latter work makes possible the separation of the contributions of different sheets of the Fermi surface to the tunneling current. The calculated gap variation is compared with that found in tunneling, acoustic attenuation, and infrared absorption experiments.

I. INTRODUCTION

THE anisotropic character of the energy gap in superconducting tin has been a frequent subject of experimental investigation. The gap variation has been determined by measuring acoustic attenuation,[1,2] electromagnetic absorption,[3] surface impedance,[4] and tunneling characteristics.[5] Efforts have been made[5,6] to associate different observed gap values with various parts of the Fermi surface. No systematic theoretical treatment has, however, been attempted.

In a recent paper[7] (I), a calculation of the anisotropic energy gap in lead was presented. The present paper consists of a semiempirical determination of the gap in tin based on some of the results and the experience gained in the previous full calculation. This approach is somewhat analogous to the recent development of the "pseudopotential theory" in calculating the properties of normal metals. A considerable effort has been expended on theoretical (first principles) calculations.[8] Such studies provide a justification for the equally useful semiempirical determination[9] of the pseudopotential from experimental data.

In the following section, we emphasize the salient features of the theory and summarize the relevant properties of the Fermi surface of tin; we also describe the requirements on an expansion of the gap in spherical harmonics imposed by the lattice symmetry. Section III consists of a determination of the expansion coefficients and a description of the gap variation over the different pieces of the Fermi surface together with a discussion of the accuracy of the procedure. The calculated gap is then compared with the results of various experiments (Sec. IV).

II. THEORY

In I, it was shown that the principal contribution to the gap anisotropy is due to the anisotropy of the phonon spectrum of the metal. That anisotropy was introduced, via a perturbation technique, into the Nambu-Górkov[10,11] equations (a generalization of the BCS[12] equation suitable for strong-coupling superconductors) in order to obtain the anisotropic energy gap. This lead gap was found in terms of an expansion in symmetrized spherical harmonics[13] (combinations of harmonics invariant under the symmetry operations of the lattice) of the form

$$\Delta(\theta,\varphi)=\sum_{i=0}^{2}\Delta_i K_i(\theta,\varphi). \qquad \text{(II.1)}$$

Here the K_i are Kubic harmonics and the angular variables refer to points on the Fermi surface displayed in the extended zone scheme. Although $\Delta(\theta,\varphi)$ is also a function of the quasiparticle energy, for the threshold phenomena of importance in most anisotropy experiments, the energy dependence can be ignored.

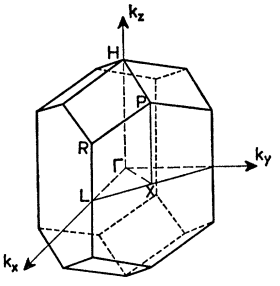

FIG. 1. The Brillouin zone of white tin.

* National Science Foundation Postdoctoral Fellow.

† Now at the General Electric Research and Development Center, Schenectady, New York.

[1] R. W. Morse, T. Olsen, and J. D. Gavenda, Phys. Rev. Letters **3**, 15 (1959).

[2] P. A. Bezuglyi, A. A. Galkin, and A. P. Korolyuk, Zh. Eksperim. i Teor. Fiz. **39**, 7 (1960) [English transl.: Soviet Phys.—JETP **12**, 4 (1960)].

[3] P. L. Richards, Phys. Rev. Letters **7**, 412 (1961).

[4] J. R. Waldram, Advan. Phys. **13**, 1 (1964).

[5] N. V. Zavaritskii, Zh. Eksperim. i Teor. Fiz. **48**, 837 (1965) [English transl.: Soviet Phys.—JETP **21**, 557 (1965)].

[6] D. H. Douglass, Jr., and L. M. Falicov, in *Progress in Low Temperature Physics*, edited by C. J. Gorter (North-Holland Publishing Company, Amsterdam, 1964), p. 172.

[7] A. J. Bennett, Phys. Rev. **140**, A1902 (1965).

[8] See, for example, V. Heine and I. Abarenkov, Phil. Mag. **9**, 451 (1964).

[9] See, for example, J. R. Anderson and A. V. Gold, Phys. Rev. **139**, A1459 (1965).

[10] Y. Nambu, Phys. Rev. **117**, 648 (1960).

[11] L. P. Górkov, Zh. Eksperim. i Teor. Fiz. **34**, 735 (1958) [English transl.: Soviet Phys.—JETP **7**, 505 (1958)].

[12] J. Bardeen, L. N. Cooper, and J. R. Schrieffer, Phys. Rev. **108**, 1175 (1957).

[13] S. L. Altmann, Proc. Cambridge Phil. Soc. **53**, 343 (1957).

The effects of the electronic-band-structure anisotropy are important only near the Brillouin-zone boundaries where the mixing of various orthogonalized plane waves (OPW's) by the crystal potential becomes considerable. If an actual electronic state $|n\rangle$ is given by

$$|n\rangle=\sum_{p\sigma} A_{np\sigma}|\mathbf{p}/\sigma\rangle, \qquad \text{(II.2)}$$

where $|\mathbf{p}/\sigma\rangle$ indicates an OPW of wave vector $\mathbf{p}$ and spin σ, then the corresponding energy gap is given approximately by the weighted average

$$\Delta_n=\sum_{p\sigma} |A_{np\sigma}|^2\Delta_p. \qquad \text{(II.3)}$$

This mixing mechanism ensures that sections of the Fermi surface in different angular sections of the extended zone scheme which coincide in the reduced zone scheme have the same energy gap.

We now describe the tin lattice symmetry, Brillouin zone, and Fermi surface characteristics which are important in the gap determination. The white-tin structure is a body-centered tetragonal lattice with two atoms per unit cell. The Brillouin zone is given in Fig. 1. The tetragonal harmonics T_i in terms of which the gap anisotropy is expanded are combinations of spherical harmonics invariant under the operations of the tetragonal group. The first four normalized harmonics are given by

$$\begin{aligned} T_0&=1.00,\\ T_1&=1.12(3Z^2-1),\\ T_2&=0.375\ (35Z^4-30Z^2+3),\\ T_3&=2.24(Z^4-2Z^2+1)\cos 4\varphi, \end{aligned} \qquad \text{(II.4)}$$

where

$$Z=\cos\theta.$$

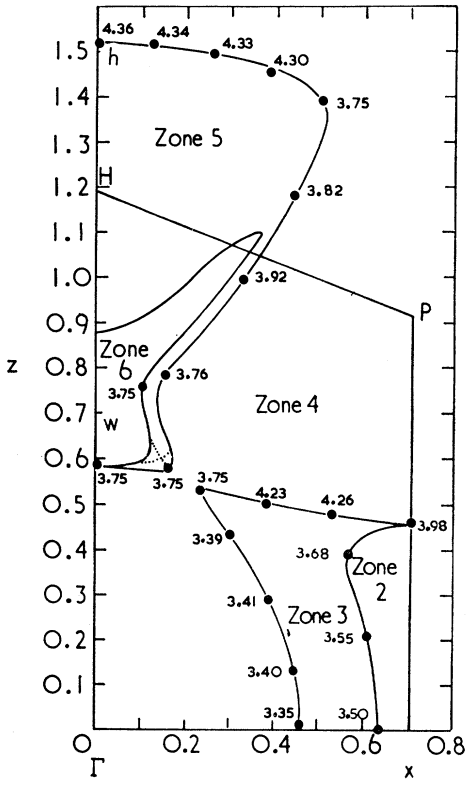

FIG. 2. A (110) cross section through Γ of the various pieces of the tin Fermi surface as calculated by Weisz (Ref. 14). The superconducting energy gap is given in units of $kT_c/2$.

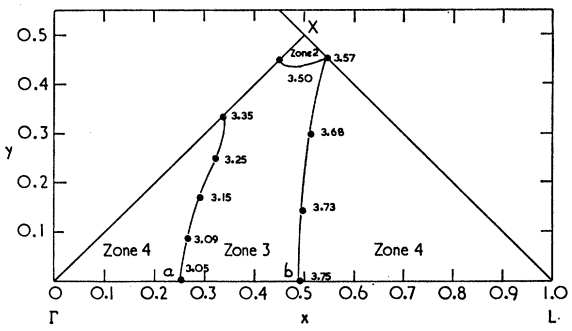

FIG. 3. A (001) cross section through Γ of the various pieces of the tin Fermi surface as calculated by Weisz (Ref. 14). The superconducting energy gap is given in units of $kT_c/2$.

A recent pseudopotential calculation by Weisz[14] has indicated significant differences between the actual Fermi surface and the predictions of the free-electron model. There are sections of the surface in the third, fourth, fifth, and sixth zones. The third zone is a hole surface of cylinders centered on the lines XP of Fig. 1; the fourth zone—a doughnut-like hole surface centered on the tetragonal axis; the fifth zone—a network of alternating pear-like surfaces centered on H with connecting pieces; the sixth zone—a small electron pocket centered on W. Cross sections of the Fermi surface in the main symmetry planes through Γ are given in Figs. 2–4.

III. DETERMINATION OF THE ANISOTROPIC ENERGY GAP

We assume that

$$\Delta(\theta,\varphi)=\Delta_0+\Delta_1T_1(\theta,\varphi)+\Delta_2T_2(\theta,\varphi)+\Delta_3T_3(\theta,\varphi), \qquad \text{(III.1)}$$

where the minimum number of terms that allow for φ variation have been included. We now determine the coefficients of this phonon-induced anisotropy from experiment, in particular, from the single-crystal tunneling work of Zavaritskii.[5]

As discussed in I, for any given crystallographic orientation of the surface, the only electrons which contribute significantly to the single-crystal tunneling characteristics are those whose velocities are within about 5° of the surface normal, i.e., those coming from

[14] G. Weisz, Phys. Rev. **149**, 504 (1966).

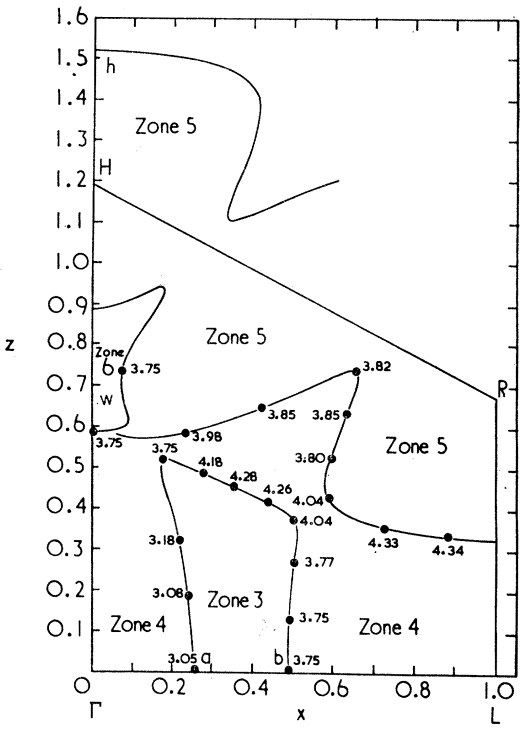

FIG. 4. A (100) cross section through Γ of the various pieces of the tin Fermi surface as calculated by Weisz (Ref. 14). The superconducting energy gap is given in units of $kT_c/2$.

a place on the Fermi surface where the normal is within about 5° of that direction. For any given tunneling direction, more than one piece of the Fermi surface may have electrons which satisfy that condition. Figure 5 is a reproduction of Zavaritskii's results expressed in the frequently used units of $kT_c/2$, where k is the Boltzmann constant and T_c is the pure bulk tin transition temperature. This is a rather inconvenient convention since the true transition temperature, also symbolized by T_c, depends on the number of impurities, etc.

In I, the constant term Δ_0 of the expansion of $\Delta(\theta,\varphi)$, which is also the average value, was set equal to the value in a dirty sample. For tin, this would correspond to 3.5 $kT_c/2$. From Zavaritskii's data, we see, however, that: (i) the average of the extremal gap values observed is approximately 3.7; (ii) the values 3.7–3.8 are the most prevalent ones. We therefore choose

$$\Delta_0=3.75.$$

In order to determine Δ_1, Δ_2, and Δ_3, we note that Zavaritskii observed the absolute maximum gap of ~4.35 in the [001] direction. He saw two gaps in the [100] direction, the absolute minimum gap of ~3.05 and a gap of about ~3.75. It is clear from Eq. (II.2) that the absolute maximum and minimum of the energy gap will occur at points on the Fermi surface where either (i) the crystal potential mixing is very small, or (ii) the OPW's which contribute to a given electronic state have wave vectors in directions which are equivalent by lattice symmetry. We confine our attention to sections of the Fermi surface whose normals are in the [100] or [001] directions. The use of a Harrison construction[15] reveals that (i) is fulfilled at the top h (Fig. 4) of the fifth-zone pear piece where the normal is in the [001] direction and at the point b (Fig. 4) on the fourth-zone surface where the normal is in a [100] direction. Condition (ii) is satisfied at the point a (Fig. 4) on the fourth-zone surface where the normal is also in a [100] direction. These are the only places on the Fermi surface where the mixing is either negligible or is among equivalent points, and the electron velocities are in the relevant symmetry directions. It is clear that the maximum value of the gap is associated with the top of the fifth-zone pear. If we can associate the gap value of 3.05 with one of the above-mentioned fourth-zone points and the gap value of 3.75 with the other, then the three anisotropy coefficients of Eq. (III.1) can be readily found.

In order to make that identification, we note that results of I have indicated that the commonly made assumption that the gap is constant on a given piece of the Fermi surface is questionable. For those pieces of the surface that subtend small angular arcs in the extended zone scheme, however, the assumption is quite good. Zavaritskii finds that the small cross-sectional area of the $\Delta=3.55$ surface in the (001) plane agrees remarkably well with the observed area of the third-zone piece of the Fermi surface. We may now distinguish

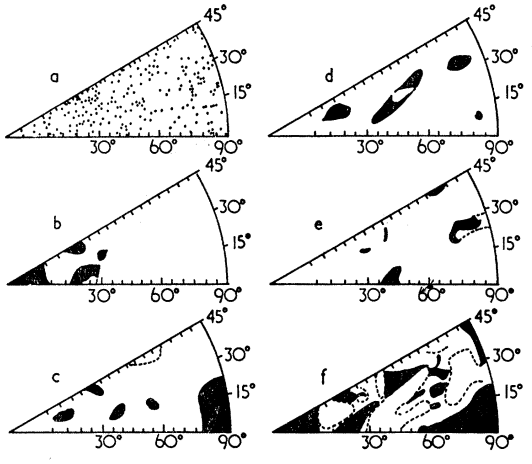

FIG. 5. A reproduction of Zavaritskii's single-crystal tunneling data plotted on a conical equiangular projection of the sphere: a, orientation of the samples used; b, regions corresponding to principal gap values of ~4.3; c, regions corresponding to principal gap values of ~3.1; d, regions corresponding to principal gap values of ~3.4; e, regions corresponding to principal gap values of ~3.55; f, regions corresponding to principal gap values of ~3.7–3.8; the dashed lines indicate the boundaries of the regions which showed no gap value of 3.7–3.8 (from Ref. 5).

[15] C. Kittel, *Quantum Theory of Solids* (John Wiley & Sons, Inc., New York, 1963), p. 258.

between the two possible identifications of the minimum gap value with one of the points a or b of the fourth-zone surface. The choice which results in anisotropy coefficients which yield a gap value Δ_{tz} closest to 3.55 for the trace of the third-zone surface in the (001) plane is the correct one. Before proceeding, it is important to emphasize again that we must distinguish between a given doublet (θ,φ) of Eq. (III.1), defined in the extended zone scheme, and any other angular coordinates associated with a corresponding piece of the Fermi surface constructed in the reduced zone scheme. If it is now first assumed that the 3.05 gap is associated with point a, then

$$\begin{aligned} 4.35&=3.75+2.24\Delta_1+3.00\Delta_2,\\ 3.05&=3.75-1.12\Delta_1+1.12\Delta_2-2.18\Delta_3,\\ 3.75&=3.75-1.12\Delta_1+1.12\Delta_2+2.24\Delta_3, \end{aligned} \quad \text{(III.2)}$$

and thus

$$\begin{aligned} \Delta_3&=+0.16,\\ \Delta_2&=-0.02,\\ \Delta_1&=+0.30, \end{aligned} \quad \text{(III.3)}$$

and

$$\Delta_{tz}=3.50.$$

If, however, the 3.05 gap is associated with point b, then

$$\begin{aligned} 4.35&=3.75+2.24\Delta_1+3.00\Delta_2,\\ 3.05&=3.75-1.12\Delta_1+1.12\Delta_2+2.24\Delta_3,\\ 3.75&=3.75-1.12\Delta_1+1.12\Delta_2-2.18\Delta_3, \end{aligned} \quad \text{(III.4)}$$

and thus

$$\begin{aligned} \Delta_3&=-0.16,\\ \Delta_2&=-0.02,\\ \Delta_1&=+0.29, \end{aligned} \quad \text{(III.5)}$$

and

$$\Delta_{tz}=3.30.$$

We conclude that the proper anisotropy coefficients are given by (III.3).

Equations (III.1) and (II.3) may now be used to obtain values of the energy gap over the entire Fermi surface. Since it is known from I that the effects of the crystal potential are important only in very small regions close to the Brillouin-zone boundaries, we confine our use of Eq. (II.3) to the actual lines of intersection of the Fermi surface with those boundaries. Furthermore, in regions where very many OPW's are mixed together, in particular at W (Fig. 2), the gap is very close to its average value. There is thus very little if any need to deal with the large number of OPW's involved in such a region. Figures 2, 3, and 4 contain, in a graphical form, values of the energy gap at various points on the Fermi surface.

We estimate the probable error involved in the use of Eqs. (III.1) and (II.3) to be considerably less than the 30% of the anisotropy probable error quoted for the full calculation of I. Our failure to use Eq. (II.3) for for all points on the Fermi surface introduces further error, in particular, in the determination of the boundaries of the regions where the mixing is very large. In addition, Zavaritskii gives his experimental data, which we use to fix the anisotropy coefficients, in a histogram-like form with an error of perhaps $\pm 10\%$ of the anisotropy. The total error, from all the above sources, in our determination of the anisotropic energy gap is about ± 0.2 $(kT_c/2)$.

TABLE I. The relative minima of the tin energy gap causing threshold structure in absorption characteristics for light propagation in each of the three main symmetry directions.

Propagation direction	Gap minima $(kT_c/2)$			
[110]	3.35	3.50	3.75	3.98
[001]	3.05	3.50	3.58	3.75
[100]	3.05	3.75	3.82	

IV. COMPARISON WITH EXPERIMENT

A. Tunneling

We first consider Zavaritskii's single-crystal tunneling data. Figure 6 is a comparison of the predicted gaps and those observed for tunneling in various directions in the (001), (100), and (110) planes. In order to predict the observed gap values, the following quantities must be known as functions of position on the Fermi surface: (1) the energy gap, (2) the direction of the electron velocity, (3) the value of the tunneling matrix element. The electron-velocity direction was taken from Weisz's calculation. Fermi-surface calculations may, however, contain small errors that radically change the the direction of the velocity vector. It was further assumed that all electrons whose velocities are within 5° of the tunneling direction contribute with equal weight, i.e., have equal tunneling matrix elements, and all other electrons make no contribution. In Zavaritskii's experiment, however, when, for a given surface direction, multiple gaps were observed with different intensities, only those causing the deepest extrema in the tunneling characteristics were tabulated. It is thus understandable that theory predicts certain gap values to be seen over larger angular regions than those indicated by Zavaritskii. The over-all agreement is reasonable, although one must remember that it is in part guaranteed by the method used to determine the anisotropy coefficients.

B. Infrared Absorption

We now compare our results with Richard's work on electromagnetic absorption. We confine our attention to the minimum energy of the radiation required to split an electron pair. It was shown in I that if

$$vq \gg \Delta_A, \quad \text{(IV.1)}$$

the relevant-energy minimum is $2\Delta_m$. Here Δ_m is the minimum value of the gap on a piece of the Fermi sur-

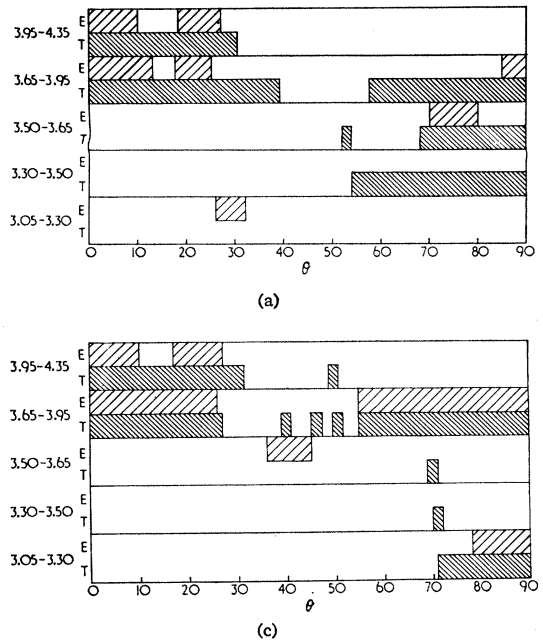

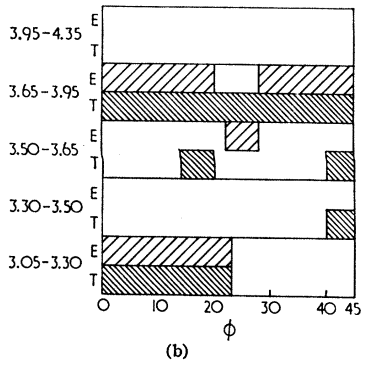

FIG. 6. A comparison of the energy-gap values (kT_c/z) observed by Zavaritskii (E) with those predicted by the present work (T) for tunneling directions in the three main symmetry planes: a, (110) plane; b, (001) plane; c, (100) plane.

face, where the electron velocity $\mathbf{v}$ is perpendicular to the photon momentum $\mathbf{q}$, and Δ_A is the effective magnitude of the anisotropic part of the energy gap, i.e.,

$$\Delta=\Delta_0+\Delta_A(\theta,\varphi). \qquad \text{(IV.2)}$$

We note that any of the various relative gap minima cause a threshold structure in the absorption curves. Condition (IV.1) is well met in tin, and thus, for a fixed direction of $\mathbf{q}$, we search along the curves $\mathbf{v}\cdot\mathbf{q}=0$ for relative minima of the gap. Table I gives the values of the threshold energy predicted by our model for radiation incident in each of the three symmetry directions. Figure 7 is a reproduction of Richard's data showing broad thresholds which are probably due to a superposition of the various minima. We note that the gap for the radiation incident in a [110] direction is significantly higher than those observed for radiation in the other two symmetry directions. Although the broad thresholds make a more quantitative comparison difficult, the data are in general accord with the results of Table I. When more complete data become available, the discussion of the absorption line shape in I will allow a detailed comparison of the present calculation with experiment.

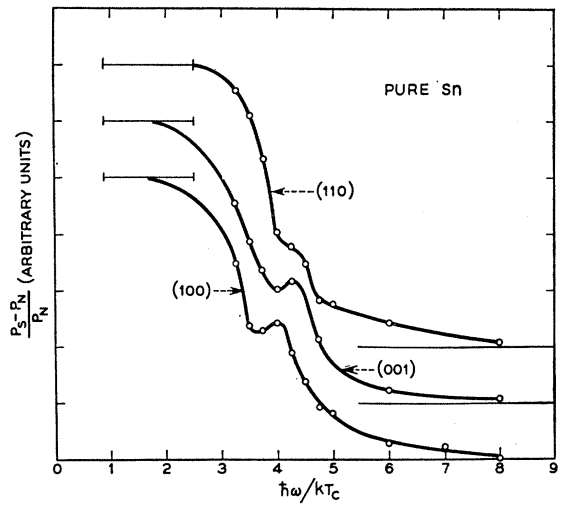

FIG. 7. Richard's acoustic-attenuation data showing the frequency dependence of the fractional difference between the power reaching the bolometer in the superconducting and normal states. The curves have been normalized for display purposes and the horizontal bar indicates the approximate band width of the lowest frequency point (from Ref. 3).

C. Acoustic Attenuation

The ratio of the attenuation in the superconducting state to that in the normal state, α_s/α_n, obtained in ultrasonic attentution experiments is usually fitted to a BCS curve of the form

$$\frac{\alpha_s}{\alpha_n}=2\left[\exp\left(\frac{\Delta(T)}{kT}\right)+1\right]^{-1}. \qquad \text{(IV.3)}$$

This has the same low-temperature behavior as Pokrovskii's expression[16]

$$\alpha_s/\alpha_n \propto \exp(-\Delta_m/kT). \qquad \text{(IV.4)}$$

Here Δ_m is the quantity defined above in connection with the infrared absorption experiments. The actual behavior of α_s/α_n is certainly more complicated than the

[16] V. L. Pokrovskii, Zh. Eksperim. i Teor. Fiz. **40**, 898 (1961) [English transl.: Soviet Phys.—JETP **13**, 628 (1961)].

TABLE II. The tin energy gap from acoustic-attenuation data.[a]

Propagation direction			Energy gap ($kT_c/2$)
θ	φ		
0°	···	[001]	3.1±0.1
90°	0°	[100]	3.5±0.1
90°	12°		4.0±0.2
90°	18°		4.3±0.2
90°	30°		4.0±0.2
90°	45°	[110]	3.8±0.1

[a] Reference 6, p. 170.

above expression and should, in fact, be proportional to a weighted average of contributions corresponding to various Δ_m's from different pieces of the Fermi surface. It is reasonable to assume, however, that the lowest gap value listed in Table I, for a given propagation direction, is the dominant one due to the exponential character of (IV.4). Table II gives some results of acoustic attenuation experiments in which the experimental curves have been fitted into a single exponential term. It is interesting to note that experiment indicates that the gap observed for propagation in the basal plane takes a maximum value of 4.3 for the $\varphi=1.8°$ direction.[2] The trace of the third-zone surface in the (100) plane through Γ is largely determined by the lattice symmetry and the nearly-free-electron character of the surface. The normals to that piece are such that it only contributes for sound-propagation directions between $\varphi=18°$ and $\varphi=45°$. It is almost certain that the discontinuity at $\varphi=18°$ accounts for the observed extremum. It is quite likely that the addition of terms in (III.1) with a φ variation more rapid than $\cos 4\varphi$ would improve the numerical agreement, in particular, for propagation directions off the symmetry axes.

ACKNOWLEDGMENTS

It is a pleasure to acknowledge stimulating conversations with Dr. L. M. Falicov, R. O. Jones, and Y. N. Rivier. I also wish to thank Dr. G. Weisz for the results of Ref. 14, prior to publication.

PHYSICAL REVIEW VOLUME 153, NUMBER 2 10 JANUARY 1967

Magnetic Properties of Superconducting Mo-Re Alloys

E. LERNER* AND J. G. DAUNT†
Ohio State University, Columbus, Ohio

AND

E. MAXWELL
National Magnet Laboratory, Massachusetts Institute of Technology, Cambridge, Massachusetts

(Received 25 March 1966; revised manuscript received 9 September 1966)

This paper gives details of research carried out on the low-temperature properties of Mo–Re alloys in the superconducting state. Measurements were made on a 52–48% alloy of Mo–Re both unannealed and annealed, the alloy being in the form of fine wires. Micrograph studies were made to determine the percentage of the various phases present in each specimen. The low-temperature measurements covered observations of the magnetization as a function of applied magnetic field at various temperatures using two different techniques. The measurements yielded the critical magnetic fields H_{c1} and H_{c2} as a function of temperature and of the state of anneal, as well as of the transition temperature T_c. Estimates were made of $H_c(T)$ and the Ginzburg-Landau-Abrikosov-Gor'kov and Maki parameters κ, $\kappa_1(T)$, and $\kappa_3(T)$. Comparisons of the results are made with results obtained previously by us from resistivity measurements on the same alloy and by other authors on similar superconducting alloys; the comparisons show consistency in the data. Our evaluations of $\kappa_1(T)/\kappa_1(T_c)$ and of $\kappa_3(T)/\kappa_3(T_c)$ are consistent with the theory of Maki.

I. INTRODUCTION

THE work reported in this paper is an extension of an investigation of the general properties of Mo–Re alloys, which has been partly reported by two of us earlier.[1] This alloy, which has the general properties of a "high-field" superconductor, was chosen because its superconductivity can be quenched in readily available fields of less than about 40 kG, and because it was desired to study the properties of the normal state also. One of the primary motivations of the work was to make a wide variety of different measurements (resistivity, thermal conductivity, magnetic moment, etc.) on actually the *same* sample of each alloy in various states of anneal. Such a study was anticipated to yield a pattern of behavior showing some inner consistency.

This paper covers the measurements of the magnetic properties of Mo–Re alloys in the form of fine wires, both annealed and unannealed. The wire was from the same spool as that used previously in the electrical and

* Present address: Physical Research Department, National Cash Register Company, Dayton, Ohio.
† Present address: Physics Department, Stevens Institute of Technology, Hoboken, New Jersey.

[1] E. Lerner and J. G. Daunt, Phys. Rev. 142, 251 (1966).